6.21

THE INFLUENCE OF BOTTOM TOPOGRAPHY ON LONG ROSSBY WAVE PROPAGATION IN THE SOUTH PACIFIC OCEAN

A. Maharaj[1], P. Cipollini[2]and N. Holbrook[3]
[1,3]Macquarie University, Sydney, Australia
[2]Southampton Oceanography Center, Southampton, United Kingdom
(Manuscript submitted to Geophysical Research Letters)

1 Introduction

Long wavelength baroclinic oceanic Rossby waves play a significant role in ocean dynamics. They maintain and influence the strong western boundary currents, are the main oceanic response to changes in atmospheric forcing and are an indicator of the length of time that anomalous conditions persist (Gill 1982). However, due to their small sea surface signature (<0.1 m) and slow propagation speeds (<0.1 m/s), detection of these waves was nearly impossible prior to the advent of satellite altimetry. With more than a decade of altimeter data from the TOPEX/Poseidon (T/P) satellite and prior missions, it is now possible to examine Rossby waves at the basin wide or global scale with centimeter accuracy. In fact, due to their westward propagation, the surface signature of Rossby waves is clearly visible in longitude-time plots (also known as Hovmöller diagrams) of sea surface height anomalies (see Fu and Chelton (2001) for a review).

Satellite observations are a particularly valuable resource in the South Pacific Ocean where *in situ* observations are scarcer than for most other oceans. One very interesting aspect of planetary wave propagation which can be investigated with satellite data is the interaction of these waves with topography. This has been suggested by a number of studies. Tokmakian and Challenor (1993) observed a change in Rossby wave characteristics when the waves crossed the mid-Atlantic ridge into the western sub-Atlantic basin. In the South Pacific Ocean, a region of enhanced SSH variability of long wavelength has been observed to be bounded by the Antarctic continent, Chile Rise, East Pacific Rise and the Pacific-Antarctic Rise (Fu and Smith 1996). Chelton and Schlax (1996) noted an increase in the amplitude of propagating sea level signals west of major topographic features in the extratropics of the world oceans. The present study investigates the long wavelength, baroclinic Rossby wave signal from 10 years of sea level anomalies in the South Pacific Ocean determined from ERS (European Remote Sensing satellite) and T/P altimeter observations.

[1]*Corresponding author address:* Angela Maharaj, Department of Physical Geography, Macquarie University, NSW 2109, Australia; email: amaharaj@penman.es.mq.edu.au

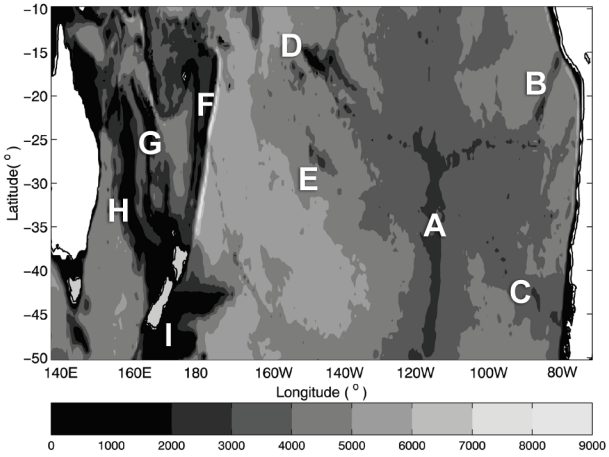

Figure 1: Smith and Sandwell (1997) bathymetry of the South Pacific Ocean. Units are in meters of depth below sea level. Labels point out major topographic features—see text for details.

2 Data

2.1 Bathymetry data

The sea floor data used here are from Smith and Sandwell (1997). The major bathymetric features of the South Pacific basin are labelled in Figure 1 and described below. In the southeast Pacific, the major feature is the East Pacific Rise (110°W—'A') which spans the meridional extent of the South Pacific Ocean to an average depth of around 2500m below sea level. Secondary ridges feature in the northeast (Nazca Ridge—'B'), southeast (Chile Rise—'C'), both at around 3000-2000m below sea level and northwest (Tuamotu Ridge at 1000m below sea level—'D') of the major ridge. South of this ridge lies the Austral seamount chain ('E').

In the southwest Pacific, the tallest and most complex bathymetric features can be found. The Kermadec Ridge (around 178°E—'F') spans the meridional extent of the basin and is separated from the Norfolk Ridge (170°E—'G') and the Lord Howe Rise (160°E—'H') by the South Fiji basin and the New Caledonia basin. South of New Zealand lies Chatham Rise ('I'). All of these features rise to less than 1000m below sea level. The topography in the southwest Pacific is of particular interest as it has the greatest density of sea mounts of any part of the world ocean floor.

2.2 MSLA data

Maps of Sea Level Anomaly (MSLA) are provided by the Developing Use of Altimetry for Climate Studies (DUACS) which is the Collecte Localisation Satellites (CLS) near real time multi-mission altimeter data processing system. MSLA are obtained from a complete reprocessing of T/P and ERS-1/2 data. There is one map every 7 days for a period of almost 10 years (14 October 1992 to 7 August 2002). T/P maps are available for that entire time period, but there are no T/P+ERS combined maps between January 1994 and March 1995 when ERS-1 was in geodetic phase. From June 1996 to February 2002, ERS-2 data are used. Details of the data processing and mapping method can be found in Le Traon and Ogor (1998) and Le Traon et al. (1998). The reader is also referred to the DUACS handbook (www.jason.oceanobs.com/documents/donnees/duacs/handbook_duacs_uk.pdf) for further details.

Maps are provided on a MERCATOR $\frac{1}{3}^{\circ}$ grid, i.e., at $\frac{1}{3}^{\circ}$ in longitude with latitude adjusted accordingly. Resolution of kilometers in latitude and longitude are thus identical and vary with the cosine of latitude (e.g., from 37 km at the equator to 18.5 km at 60°N/S). Units are in centimeters. This study focuses on the South Pacific Ocean from 10°S to 50°S.

3 Method

The two-dimensional Radon Transform (2D-RT) is a tool commonly used in image analysis that can be utilized to determine an objective estimate of the orientation of lines in a Hovmöller plot in order to objectively calculate the speed of the dominant signal in the image. It is a projection of the image intensity along a radial line oriented at a specific angle, θ (Deans 1983, Challenor et al., 2001). Alignments of the data at an angle in longitude-time space are lines of constant speed. When θ is orthogonal to the direction of the alignments in the plot, the Radon energy is maximum. Computing the RT of a Hovmöller for different values of θ, and then its energy, allows one to find the value of θ for which the energy is maximum. This objectively determines the angle of the predominant energy signal in the data. The corresponding speed can then be readily calculated from θ from simple trigonometric considerations, being proportional to tan(θ). The 2D-RT is typically used only to determine the speed of the dominant signal, corresponding to the energy maximum. Here we also examine how the energy is distributed through the different values of θ, which can indicate characteristics of wave activity such as the presence of a waveguide as shown by Cipollini et al. (1999).

Longitude-time series were extracted from the MSLA dataset for every 1° of latitude with a 20° longitude running window from 10°S to 50°S. Windows or data blocks with land were filled with a Gaussian interpolation scheme if the gap width was less than 10% of the window. Otherwise, the land was left in. Spikes and outliers in the dataset were identified as more than three standard deviations away from the mean and removed. These data were then Gaussian interpolated. The two dimensional Gaussian interpolation scheme places greater emphasis on space than in time because it is expected that the values will be more closely related in space. The full-width half maximum (FWHM) and search radius were set to $\frac{2}{3}^{\circ}$ and 1° in space and 1.4 days and 7 days in time.

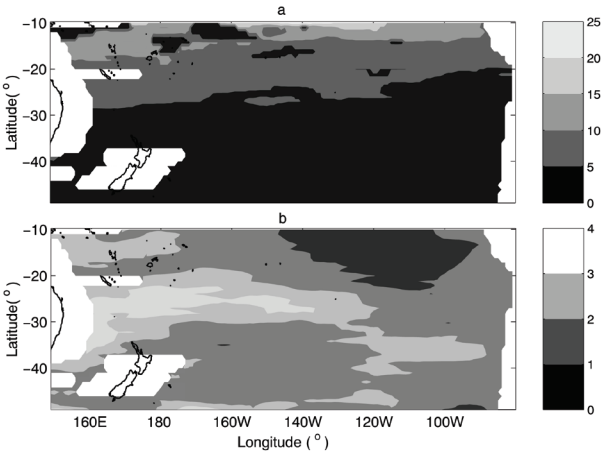

Figure 2: (a) Westward propagating phase speeds (cm/s) and (b) the corresponding maximum standard deviation of Radon Transform energy (arbitrary units). White areas are not included due to the presence of land in the analysis window.

Each window or data block is zero padded and passed through what we refer to as the 'westward-only' filter (Cipollini et al., 2001). This filter removes stationary and eastward propagating signals (the second and fourth quadrants in wavenumber frequency space) leaving only westward propagating signals (the first and third quadrants). This effectively also removes the annual standing signal. Additionally, a few more spectral bins around the annual peak are forced to zero to effectively remove any stationary quasi-annual signal. The 2D-RT was then calculated for each longitude-time series for θ ranging from 0°- 90° (every 1°).

4 Results and discussion

Figure 2 shows the westward phase speeds (in cm/s) from the RT analysis of the filtered data for the South Pacific. In general, the phase speeds are faster in the lower latitudes (∼25cm/s at 10°) and decrease polewards (∼2cm/s at 50°S). There is also some indication of an increase in speed on the western side of the basin in the mid-latitudes thought to be indicative of thermocline deepening in the west (Chelton and Schlax, 1996). However, north of 20°S, particularly in the mid to western basin, are some anomalously low speeds that stretch over approximately 10° of longitude.

Figure 3 shows the RT angle of maximum energy, θ_{max}, from the Radon analysis overlayed with contours of bathymetry from Smith and Sandwell (1997). As expected, in general, θ_{max} is higher at lower latitudes (faster propagation) and decreases polewards (slower propagation). The

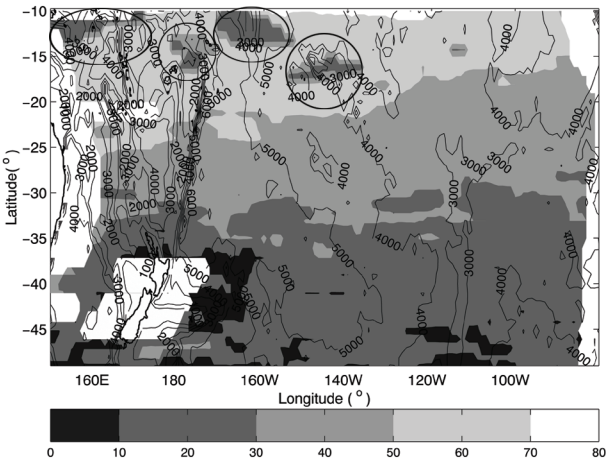

Figure 3: The dominant angle (θ) of propagation (°) found from the 2D-RT analysis overlayed on contours of bathymetry from Smith and Sandwell (1997). The circled features are regions of anomalously low propagation angles

large regions of anomalously slow speeds in Figure 2 are shown to have significantly small angles relative to their surroundings (circled features in Figure 3). The contour overlay of the bathymetry shows that these regions correspond to steep gradients (changes in height of 4000m-5000m in around 10° of longitude) of sea floor topography. A large region of very small angles can also be seen west of 160°W between 36°S and 45°S. Between 160°W to 170°W and 20°S to 35°S, the angle (and speed) increases over deeper water.

These features display a negative relationship between phase speed (or the dominant angle as an indicator for phase speed) and bathymetry that concurs with theoretical knowledge. It is expected that the waves will propagate faster in deeper water and slower in shallower water. However, there is no clear indication of slower propagation speeds over the ridge systems or over the entire western Pacific which is dominated by high topography. Also, it is apparent that the critical factor in the slow down is not the slope since the steepest feature in the basin, the Kermadec Ridge, does not show this characteristic. However, the topographic features over which the anomalous speeds occur are not only relatively steep (around a change in height of 1m for every 100m) but also relatively isolated from other topographic features or surrounded by deeper basins. Hence, it is more likely that topographic steering is taking place, deviating the Rossby wave energy around these features.

Figure 4 shows the standard deviation of the RT energy (arbitrary units) from selected meridional transects plotted against the possible range of angles (θ). The panels are selected frames from a movie scanning from east to west (since the data have been filtered to examine westward propagating features) across the South Pacific basin. Superimposed on the plots are a solid line and dots indicating angles for first baroclinic mode Rossby waves traveling at theoretical speeds and at perturbed speeds, respectively(Killworth and Blundell 2003a,b). The latter consists of model results which include the effects of the baroclinic

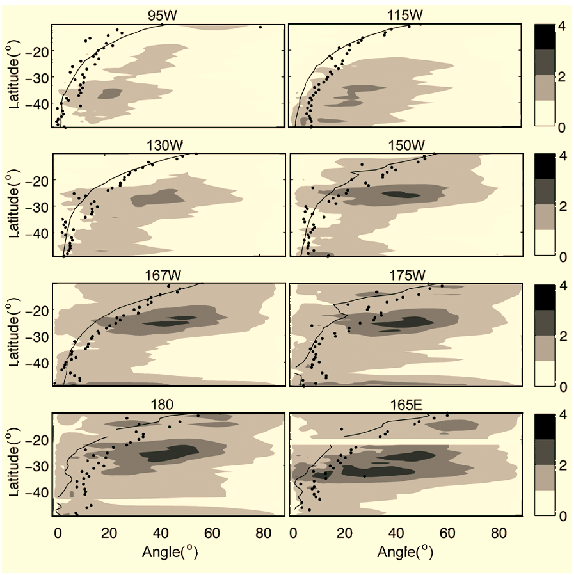

Figure 4: Standard deviation of RT energy (arbitrary units) for angles between 0° and 90° for selected meridional transects across the South Pacific. Solid lines and dots indicate theoretical and perturbed speed estimates, respectively, from Killworth and Blundell (2003a,b).

background mean flow and 1° resolution bathymetry.

The signal with maximum standard deviation (i.e., greatest variability) tilts to the right. That is, equatorwards, the peaks in the RT are at higher angles (faster speeds), while polewards the peaks are at lower angles (slower speeds). The energy in the western side of the basin is significantly different to that on the eastern side. In the southeast Pacific, the energy is weak, and constrained to a narrow range of angles. Progressing westwards, the energy intensifies, the range of angles widens.

At the eastern boundary (95°W), the signal has low intensity everywhere with only a small maxima around 25°S and 35°S. As the signal crosses the East Pacific Rise (∼112°W), it expands south and extends from 25°S to 45°S (115°W). This range corresponds well to the main peak of the East Pacific Rise. After crossing the ridge, the signal extends north and breaks into two maximas around 130°W with the major signal seen between 25°S and 30°S. This is near the eastern edge of the Tuamotu ridge. Although it is not perfectly clear, from 150°W to 175°W, it seems that the minor peak spreads south and intensifies.

West of 130°W, the major peak intensifies and extends northwards till around 167°W. The peak maximum is now between 20°S and 27°S. Movement of the signal here coincides with the passage between the Tuamotu ridge and the Austral sea mounts. This energy appears to be veered northwards by the ridges and sea mounts in the region. Between 175°W and 180°, near the Kermadec ridge, variability increases almost everywhere (every latitude) and over a large range of angles. Then the major peak starts to move south. Through 165°E and 160°E, over the Lord Howe Rise, the peak intensifies and angles with maximum variability further increase in range. It is also apparent that of-

ten, particularly where the energetic variability is greatest, the dominant signal is faster than both linear and perturbed estimates.

These series of plots show meridional movement of the energy that corresponds with the wave negotiating and interacting with bathymetry. Further, there appears to be a dominant band of energetic variability between 20°S and 30°S west of the East Pacific Rise with a region of high variability in SSH and high angles between these latitudes. The interaction of westward propagating Rossby waves with the unique bathymetry of the South Pacific Ocean clearly seems to be steering Rossby waves between the Tuamotu Ridge and the Austral seamounts. Rossby wave propagation speeds slow down north of 20°S, thus contributing to the formation of a waveguide in the subtropics. Figure 4 shows a significant increase in the standard deviation of the energy in the presence of ridges and seamounts. Additionally, a wider range of angles become significant. This suggests that the signal breaks into varying speeds that may be equally dominant and may be indicative of multiple topographically modified baroclinic modes. Such a process has been suggested to occur in the western South Pacific (Heath, 1985) and alluded to by Chelton and Schlax (1996) in their observations of an increase in wave amplitude west of oceanic ridges. Therefore it may be important to examine the secondary energy peaks in the Radon Transform analysis.

5 Summary and conclusion

This study has examined the long wavelength, westward propagating, baroclinic Rossby wave signal from 10 years of filtered, westward propagating only, sea level anomalies in the South Pacific Ocean. Application of the two-dimensional Radon Transform analysis to the sea level anomalies has provided estimates for the first baroclinic wave phase speed as well as estimates of the wave energy characteristics throughout the basin.

The authors speculate that in the presence of a steep but isolated topographic feature, westward propagating Rossby waves may be steered so that the observed energetic variability and propagation speeds over these features are small. This is seen over four topographic features north of 20°S in the South Pacific. However, in the presence of a long, meridional ridge system, westward propagating Rossby waves must travel over the ridge. This may lead to topographically modified baroclinic modes or a surface amplification of higher order modes. This would account for the increase in the energetic variability and the large range of dominant angles observed over ridge systems such as the Kermadec Ridge and Lord Howe Rise. The interaction of westward propagating Rossby waves with the unique bathymetry of the South Pacific appears to be contributing towards the formation of a waveguide in the subtropics. These assertions are currently being investigated.

Acknowledgments The altimeter products were produced by the CLS Space Oceanography Division as part of the Environment and Climate EU ENACT project (EVK2-CT2001-00117) and with support from CNES. The authors would like to thank Peter Killworth and Jeff Blundell for providing the perturbed speed estimates. A large portion of this work was carried out during A. Maharaj's visit to Southampton Oceanography Centre, UK. A. Maharaj is supported by an Australian Postgraduate Award.

References

Challenor, P. G., P. Cipollini and D. Cromwell, 2001: Use of the 3D Radon Transform to examine the properties of oceanic Rossby waves, *J. Atmos. Oceanic Technol.*, **18**, 1558–1566.

Chelton, D. B., and M. G. Schlax, 1996: Global observations of oceanic Rossby waves, *Science*, **272**, 234–238.

Cipollini, P., D. Cromwell, P. G. Challenor and S. Raffaglio, 2001: Rossby waves detected in global ocean colour data, *Geophys. Res. Lett.*, **28**(2), 323–326.

———, ———, M. S. Jones, G. D. Quartly and P. G. Chellenor, 1997: Concurrent altimeter and infrared observations of rossby wave propagation near 34°N in the Northeast Atlantic, *Geophys. Res. Lett.*, **24**, 885–892.

———, ———, G. D. Quartly and P. G. Challenor, 1999: Observations of Rossby wave propagation in the northeast atlantic with TOPEX/POSEIDON altimetry, *Advances in Space Research*, **22**(11), 1553–1556.

———, G. D. Quartly, P. G. Challenor, D. Cromwell and I. S. Robinson, 2004: *Manual of Remote Sensing*, chapter Remote sensing of extra-equatorial planetary waves in the oceans.

Deans, S. R., 1983: *The Radon transform and some of its applications*, John Wiley.

Fu, L. L., and D. B. Chelton, 2001: *Satellite Alitmetry and Earth Sciences*, chapter Large scale ocean circulation, pp. 133–169, Academic Press.

———, and R. D. Smith, 1996: Global ocean circulation from satellite altimetry and high-resolution computer simulation, *Bull. Am. Meteorol. Soc.*, **77**, 2625.

Gill, A. E., 1982: *Atmosphere-ocean dynamics*, Academic Press, Inc, 662pp.

Heath, R. A., 1985: A review of the physical oceanography of the seas around New Zealand - 1982, *N. Z. J. Mar. Freshwater Res.*, **19**, 79–124.

Hill, K. L., I. S. Robinson and P. Cipollini, 2000: Propagation characteristics of extratropical planetary waves observed in the atsr global sea surface temperature record, *J. Geophys. Res.*, **105**, 21927–21945.

Killworth, P. D., and J. R. Blundell, 2003a: Long extra-tropical planetary wave propagation in the presence of slowly varying mean flow and bottom topography. I: the local problem, *J. Phys. Oceanogr.*, **33**, 784–801.

———, and ———, 2003b: Long extra-tropical planetary wave propagation in the presence of slowly varying mean flow and

bottom topography. II: ray propagation and comparison with observations, *J. Phys. Oceanogr.*, **33**, 802–821.

Smith, W. H. F., and D. T. Sandwell, 1997: Global sea floor topography from satellite altimetry and ship depth soundings, *Science*, **277**(26), 1956–1962.

Tokmakian, R. T., and P. G. Challenor, 1993: Observations in the Canary Basin and the Azores Frontal Region using Geosat data, *J. Geophys. Res.*, **98**, 4761–4773.

Traon, P. Y. L., F. Nadal and N. Ducet, 1998: An improved mapping method of multi-satellite altimeter data, *J. Atmos. Oceanic Technol.*, **25**, 522–534.

———, and F. Ogor, 1998: Ers-1/2 orbit improvement using topex/poseidon: the 2 cm challenge, *J. Geophys. Res.*, **103**, 8045–8057.